SKB

TECHNICAL REPORT 94-25

Kinetic modelling of bentonite-canister interaction

Long-term predictions of copper canister corrosion under oxic and anoxic conditions

Paul Wersin, Kastriot Spahiu, Jordi Bruno

MBT Tecnología Ambiental, Cerdanyola, Spain

September 1994

SVENSK KÄRNBRÄNSLEHANTERING AB
SWEDISH NUCLEAR FUEL AND WASTE MANAGEMENT CO

BOX 5864 S-102 40 STOCKHOLM
TEL. 08-665 28 00 TELEX 13108 SKB
TELEFAX 08-661 57 19

KINETIC MODELLING OF BENTONITE-CANISTER INTERACTION

LONG-TERM PREDICTIONS OF COPPER CANISTER CORROSION UNDER OXIC AND ANOXIC CONDITIONS

Paul Wersin, Kastriot Spahiu, Jordi Bruno

MBT Tecnología Ambiental, Cerdanyola, Spain

September 1994

Kinetic modelling of bentonite - canister interaction. Long-term predictions of copper canister corrosion under oxic and anoxic conditions.

Paul Wersin, Kastriot Spahiu, Jordi Bruno

MBT Tecnología Ambiental, Cerdanyola, Spain

September 1994

Key words: Cu corrosion, kinetics, diffusion, time scales

Abstract (English)

A new modelling approach for canister corrosion which emphasises chemical processes and diffusion at the bentonite-canister interface is presented. From the geochemical boundary conditions corrosion rates for both an anoxic case and an oxic case are derived and uncertainties thereof are estimated via sensitivity analyses.

Time scales of corrosion are assessed by including calculations of the evolution of redox potential in the near field and pitting corrosion. This indicates realistic corrosion depths in the range of 10^{-7} and $4 \cdot 10^{-5}$ mm/yr, respectively for anoxic and oxic corrosion. Taking conservative estimates, depths are increased by a factor of about 200 for both cases. From these predictions it is suggested that copper canister corrosion does not constitute a problem for repository safety, although certain factors such as temperature and radiolysis have not been explicitely included. The possible effect of bacterial processes on corrosion should be further investigated as it might enhance locally the described redox process.

Abstract (Swedish)

En ny metod för modellering av kapselkorrosionen, som betonar kemiska processer och diffusion vid gränsytan mellan bentonit och kapsel presenteras. Från de geokemiska gränsvillkoren härleds corrosionshastigheter för både ett icke-oxiderande och ett oxiderande fall och osäkerheterna i dessa uppskattas genom känslighetanalyser.

Tidskalan för korrosionen fastställs genom att innefatta beräkningar av redoxpotentialen i närområdet och gropfrätning. Detta visar på realistiska korrosionsdjup i området 10^{-7} respektive $4 \cdot 10^{-5}$ mm/år för korrosion under reducerande respektive oxiderande förhållanden. Vid konservativa uppskattningar ökar djupen med en faktor på 200 i båda fallen. Dessa förutsägelser tyder på att korrosion av kopparkapseln inte utgör ett problem för förvarets säkerhet, även om vissa faktorer som temperatur och radiolys inte explicit inkluderats. Den möjliga effekten av bakteriella processer på korrosionen bör utredas ytterligare eftersom de lokalt kan höja den beskrivna redoxprocessen.

Table of materials

1 Introduction

The prediction of the life time of a canister in a HLW repository still constitutes a difficult task. Among the various factors which may contribute to degradation of the material, chemical corrosion is of particular importance. Chemical corrosion strongly depends on the geochemical conditions of the near field, i.e., the dissolved constituents in the surrounding bentonite buffer. In the current canister design (SKB 91), a copper container of 5 cm thickness (including an inner lead mantle) is envisionned. Thus, the chemical interaction of copper with the clay porewater will drive the corrosion process. The extent of this process is in principle determined by the chemical reactivity at the copper surface and the mass transfer from and to this surface.

In view of the lack of experimental data, previous work has used very simple approaches to estimate the impact of copper corrosion. Thus, from thermodynamic calculations (KBS-3; The Swedish Corrosion Research Institute, 1983; Wersin et al., 1993) it could be shown that alteration products of Cu are stable and that the corrosion process is expected to be affected by the redox conditions of the clay medium. On the other hand, with aid of simple transport-related calculations (Neretnieks, 1983); a range of possible fluxes of degrading agents, such as O_2 and HS^- could be derived and conservative estimates of upper corrosion rates deduced thereof. Very few attempts, however, have been made to link transport with chemical processes. Recently, we have reviewed (Wersin et al., 1993) experimental, archeological, and geological data related to canister corrosion and proposed a simple box-model for assessing long-term corrosion rates. The model included thermodynamic and kinetic processes and flow under steady-state conditions. Application of the model to Cu corrosion in anoxic medium allowed crude estimates of possible Cu fluxes.

In this work we extend the modelling approach by introducing a multi-box system which includes diffusion as the main transport component. We reevaluate boundary conditions for anoxic corrosion and derive realistic corrosion rates. We further assess corrosion under oxic conditions using a similar procedure. Finally, we estimate time scales of corrosion by taking into account sensitivity analyses performed with the model and uncertainties related to other factors (e.g., pitting corrosion). A major point in the time scale assessment is the redox potential (Eh) which is the most critical chemical variable controlling corrosion. Therefore, we specifically include the impact of changing Eh in the repository by taking into account O_2 and Eh time-dependence in the clay medium (Wersin et al., 1994).

2 Thermodynamic boundary conditions

Porewater chemistry in the bentonite medium is relatively well understood in term of major ion composition (Snellman, 1984; Wanner et al., 1992). Thus, pH conditions are expected to be controlled by calcite equlibrium and ion-exchange reactions occuring at the clay/water interface. Eh is expected to vary with time and to evolve from oxic to anoxic conditions. A convenient way for assessing thermodynamic boundary conditions for copper species is to visualize their stability field in a Eh-pH or a pe-pH diagram. Such a diagram, calculated for expected chemical conditions in the bentonite, is shown in Fig. 1. Under oxic conditions, malachite, a Cu(II) hydroxy carbonate, is expected to form through the corrosion process. Under anoxic conditions, copper sulphides are stable as a result of the strong affinity of Cu(I) and Cu(II) for the sulphide ligand. Note that a small stability field of native copper is predicted at intermediate Eh.

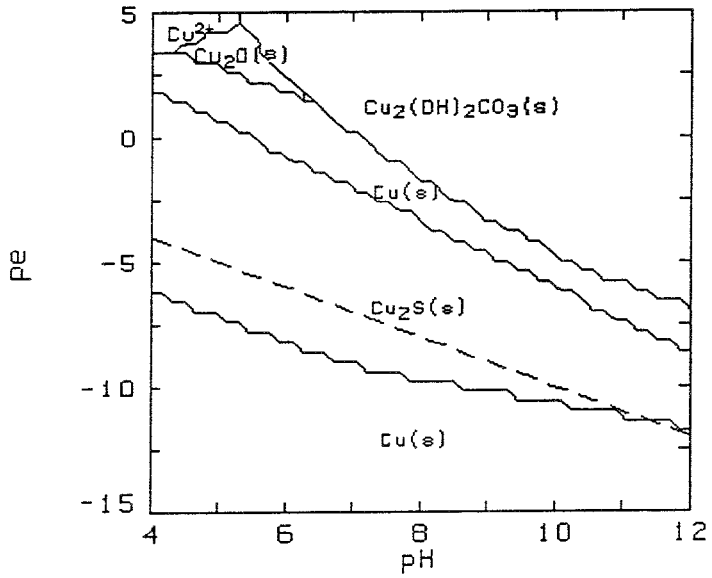

Fig. 1 Predominance diagram showing pe-pH range for main Cu species under relevant chemical conditions in the compacted clay medium with $[CO_3]_t = 10^{-3}$ M, $[S]_t = 10^{-6}$ M, [Cu] = 10^{-4} M.

3 Model concept

3.1 Single-box vs multi-box model

In an earlier report (Wersin et al., 1993) we have outlined the concept of a kinetic modelling approach for long-term canister corrosion based on the STEADYQL algorithm (Furrer et al., 1989).

The code, in its original version, formulates fast processes as equilibrium reactions and slow processes in the form of empirical rate laws for a single flow-through reactor at steady state. We applied this "single-box" model to the bentonite-copper system in order to evaluate the limiting conditions for the corrosion rates of the copper canister. Since the component fluxes are determined by the imposed constant flow velocity, this single-box approach does not account for the diffusive mass transfer which, however, is the dominant transport process in the compacted clay. Therefore, in order to assess realistic corrosion rates, we suggested the use of the "multi-box" model based on a recently developed extended version of STEADYQL (Furrer and Wehrli, 1992) which includes the diffusive flux of all dissolved species. In this report we adapt this diffusion-extended code to the assessment of long-term canister corrosion under repository conditions.

The principles of this approach are schematically illustrated in Fig. 2. The two boundary compartments are regarded as infinite reservoirs of fixed composition. In the model discussed here, they represent the bentonite medium and the copper canister, respectively. Diffusion in and out of these compartments constitutes the dominant transport process. Flow may occur along the canister - bentonite boundary. In the centre, at a given diffusion distance from the bulk clay and the bulk canister surface, chemical reactions among the components occur. These include equilibrium reactions as well as kinetically-controlled processes, such as corrosion. The system is constrained by its spatial and temporal invariability and thus represents steady-state conditions.

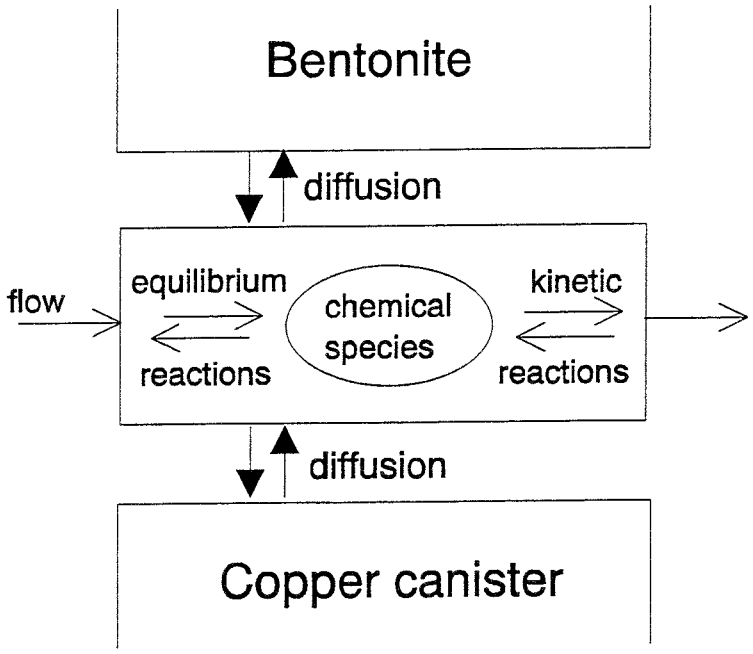

Fig. 2 Scheme of corrosion model which is based on diffusion-extended version of STEADYQL code. Partly adapted from Furrer and Wehrli (1992).

3.2 Mathematical formulation

Here a formulation in a general format is given which allows to define the system of interest. From the definitions set below, the system at steady state can be expressed by few constraints with regard to the choice of components, species, and expression for fluxes and reaction rates. The mathematical description presented here closely follows the one given by Furrer et al. (1989).

3.2.1 Mass action equations

Equilibrium reaction involving dissolved and solid species are defined by the mass action equation which in the general algebraic form can be written as:

$$C(i) = K(i)\prod_j X(j)^{a(i,j)} \tag{1}$$

where C(i) is the molar concentration of species i, K(i) is the conditional stability constant, X(j) is the free concentration of the component j, a(i,j) is the stoichiometric coefficient of component j in species i. Eq. (1) is defined by either fixing the total concentration of j or by fixing the free concentration (or activity) of X(j) such as for example pH or the activity of a solid phase.

3.2.2 Rates of slow processes and fluxes

For any slow process the rate is expressed as:

$$R(l) = \prod_m P(m)^{w(l,m)} \prod_i C(i)^{n(l,i)} \tag{2}$$

where R(l) is the rate of process l [mol dm^{-2} s^{-1}], P(m) is the value of parameter m, w(l,m) is the exponent of parameter m in process l, and n(l,i) is the exponent of parameter m of the concentration of species i.

The flux J(l,j) of a component j due to process l is:

$$J(l,j) = R(l)s(l,j) \tag{3}$$

where s(l,j) is the stoichiometric coefficient of component j in process l. Eq. (3) is valid for all slow processes. For practical reasons, the fluxes due to chemical processes are separated from the ones due to outflow and, in the case of the diffusion-extended version of STEADYQL, also from the diffusive fluxes. Thus, for a slow chemical process, the flux is expressed as:

$$J(l^0, j) = s(l^0, j) \prod_m P(m)^{w(l,m)} \prod_i C(i)^{n(l,i)} \quad (3a)$$

where 1^0 represents a chemical process.

In the diffusion-extended version of the STEADYQL code the diffusive flux of a component between adjacent compartment is included:

$$J(diff, j', t \leftrightarrow u) = \sum_{i'} J(i', j', t \leftrightarrow u) \quad (3b)$$

where J(i',j',t↔u) is the diffusive flux of a mobile species i' of component j between compartment t and u. The diffusive flux of each mobile species is expressed according Fick's first law and separated into two processes:

$$J(i', j', t \leftrightarrow u) = \frac{D(i')}{\Delta x(t,u)} c(i', u) - \frac{D(i')}{\Delta x(t,u)} c(i', t) \quad (3b')$$

where D(i') is the diffusion coefficient of species i' [$dm^2\ s^{-1}$], Δx(t,u) is the diffusion distance [dm] between compartment t and u and c(i',t), c(i,u) are the free concentration of i' in compartments t and u, respectively.

The flux due to outflow for any mobile component j'' is:

$$J(out, j'') = -v \sum_{i''} a(i'', j'') C(i'') \quad (3c)$$

where v is the outflow velocity [dm s^{-1}] and a(i'',j'') is the stoichiometric coefficient of species i''.

3.2.3 Flux balance and mole balance

Both flux balance and mole balance are formulated as difference functions, which must be zero when the conservation conditions are satisfied. For the immobile components, such as surface components, the mole balance equation is:

$$Y(j^*) = \sum_{i^*} a(i^*, j^*) C(i^*) - T(j^*) = 0 \quad (4)$$

where Y(j*) is the difference function for any immobile component j*, T(j*) is the total concentration of the component.

For any mobile component the sum of all fluxes must be zero at steady-state:

$$Y(j'') = \sum_{l} J(l, j'') = 0 \qquad (5)$$

where Y(j") is the difference function for any mobile component j".

The difference functions Y(j*) and Y(j") are solved via iteration by the code until convergence, set by the convergence criterium, for the difference functions Y(j*) and Y(j") is reached. The algebraic formulation (Eqs. (1)-(5)) is expressed in the form of matrices in the STEADYQL algorithm (see Furrer et al., 1989).

3.3 Applications

The application of the STEADYQL code offers a relatively simple, yet mechanistic model for the description of virtually any geochemical system. It should be noted that rather detailed chemical information of the solute and solid matrix together with basic transport characteristics are required for adequate description of the system. Models of this type have been successfully applied to very distinct geochemical problems, such as the prediction of proton fluxes in soil systems (Furrer et al., 1990), redox processes at the oxic-anoxic boundary in a lake (Furrer and Wehrli, 1992), or the water-rock interactions controlling metal release in a copper mine (Strömberg and Banwart, 1994).

In the context of near-field modelling, prediction of long-term effects of the chemical stability of the respository constitutes an important task. Under these conditions the use of a robust kinetic model, based on steady-state and the appropriate geochemical boundary conditions, is particularly useful. Since solute transport in the compacted clay is expected to be dominated by a steady transport regime dominated by diffusion, the diffusion-extended version of the STEADYQL code (see above two sections) offers a realistic geochemical description of slow, kinetically-driven processes. Thus, even in cases where adequate experimental data is lacking, such as copper canister corrosion, quantitative information can be gained from the appropriate boundary conditions. In particular, different test cases can be performed, including the comparison between diffusion-limitation vs chemical reaction limitation. The following case studies provide examples of the usefulness of this modelling approach in assessing realistic time scales of canister corrosion.

4 Modelling copper canister corrosion

4.1 Anoxic corrosion of Cu

4.1.1 Boundary conditions

The geochemical constraints are given by the thermodynamic boundary conditions (section 2) of the bentonite medium and the kinetics of the corrosion process at the copper-bentonite interface. In the STEADYQL modelling concept it is convenient to define a "reference case" which constitutes a realistic estimate of the geochemical constraints and from that perform a sensitivity analysis of the key parameters. The description of the system for a reference case is performed subsequently by separation into fast and slow processes.

Fast processes: These are defined by equilibrium reactions between an arbitrary selection of components and their stability constants according to Eq. (1). From the equilibrium chemistry modelling studies of the bulk bentonite system (Wanner, 1986; Wanner et al., 1992) interactions between the components H^+, CO_3^{2-}, SO_4^{2-}, HS^-, Ca^{2+}, Fe^{2+}, Fe^{3+}, plus Cu^{2+} are described by complexation reactions in the porewater and solid equilibria as shown in Table 1. The following solid equilibria are imposed.

$$CaCO_3(s) + H^+ = Ca^{2+} + HCO_3^- \quad (6)$$

$$Fe(OH)_3(s) + 3H^+ = Fe^{3+} + 3H_2O \quad (7)$$

$$FeS(s) + H^+ = Fe^{2+} + HS^- \quad (8)$$

$$CuS(s) + H^+ = Cu^{2+} + HS^- \quad (9)$$

The assumption of calcium carbonate equilibrium is inherent from the thermodynamic bentonite model which considers calcite impurities in the clay. This equilibrium largely controls proton, alkalinity, and calcium fluxes. In addition, however, experimental data (Werme (unpubl.), 1988; Wanner et al., 1992) indicate that ion exchange and acid/base reactions at the clay surface affect solution composition. For the purpose of this modelling exercise this effect can be accounted for by fixing the pH in the limiting compartments at about 9.0 which is in agreement with the experimental data. Ferric hydroxide, a further common impurity in the clay is known to persist over long time periods in anoxic sediments (Berner, 1971). Therefore, release of Fe^{3+} from to the porewater is considered by fixing ferrihydrite equilibrium (Eq. (7)) in the bentonite compartment. The upper concentration range of dissolved sulphide is fixed by amorphous FeS equilibrium (Berner, 1971; Eq. (8)) in the bentonite compartment and thus represents the condition of maximum possible flux of HS^- to the copper canister. The release of Cu in anoxic medium is thermodynamically constrained by the formation of insoluble copper sulphide (section 2). For conservative reasons, equilibrium with CuS (Eq. (9)), which is slightly more soluble than Cu_2S is

Table 1 Stoichiometry of fast processes with equilibrium constant and diffusivities (anoxic case)

Reaction		logK	source	[6]diffusivity $1 \cdot 10^{-7} * cm^2 s^{-1}$
Aqueous phase:				
H^+	= H^+	0		6.27
CO_3^{2-}	= CO_3^{2-}	0		0.50
HS^-	= HS^-	0		1.21
Cu^{2+}	= Cu^{2+}	0		0.41
Fe^{2+}	= Fe^{2+}	0		0.41
Ca^{2+}	= Ca^{2+}	0		0.42
Fe^{3+}	= Fe^{3+}	0		0.20
Cu^+ [7]	= Cu^+	0		0.50
$H_2O - H^+$	= OH^-	-14.00	1	3.17
$CO_3^{2-} + 2H^+$	= H_2CO_3	16.68	1	1.20
$CO_3^{2-} + H^+$	= HCO_3^-	10.33	1	0.71
$HS^- + H^+$	= H_2S	7.02	1	1.56
$Cu^{2+} - H^+$	= $Cu(OH)^+$	-8.00	1	1.00
$Cu^{2+} - 2H^+$	= $Cu(OH)_2$	-16.20	1	1.00
$Cu^{2+} - 3H^+$	= $Cu(OH)_3^-$	-26.30	1	1.00
$Cu^{2+} + CO_3^{2-}$	= $CuCO_3$	6.77	1	0.32
$Cu^{2+} + 2CO_3^{2-}$	= $Cu(CO_3)_2^{2-}$	10.10	1	0.32
$Cu^{2+} + CO_3^{2+} + H^+$	= $CuHCO_3^+$	14.62	1	0.45
$Fe^{2+} + CO_3^{2-}$	= $FeCO_3$	5.50	2	0.32
$Fe^{2+} + 2CO_3^{2-}$	= $Fe(CO_3)_2^{2-}$	7.00	2	0.32
$Ca^{2+} + CO_3^{2-}$	= $CaCO_3$	3.22	1	0.34
$Ca^{2+} + CO_3^{2-} + H^+$	= $CaHCO_3^+$	11.44	1	0.45
$Fe^{3+} - H^+$	= $Fe(OH)^{2+}$	-2.19	1	0.60
$Fe^{3+} - 2H^+$	= $Fe(OH)_2^+$	-5.67	1	1.00
$Fe^{3+} - 3H^+$	= $Fe(OH)_3$	-13.09	1	1.00
$Fe^{3+} - 4H^+$	= $Fe(OH)_4^-$	-21.60	1	1.00
$Fe^{3+} + CO_3^{2-} - H^+$	= $FeOHCO_3$	3.83	3	0.32
$Fe^{3+} + 2CO_3^{2-}$	= $Fe(CO_3)_2^+$	7.40	3	0.32
$Cu^+ + 2Cl^-$ [7]	= $CuCl^-$	5.50	1	1.90
$Cu^+ + 3Cl^-$ [7]	= $CuCl_3^{2-}$	5.70	1	1.90
Solid phase:				
$Ca^{2+} + CO_3^{2-}$	= $CaCO_3$	8.48	1	
$Fe^{3+} + 3H_2O - 3H^+$	= $Fe(OH)_3$	0.4	4	
$Fe^{2+} + HS^- - H^+$	= FeS	2.95	5	
$Cu^{2+} + HS^- - H^+$	= CuS	22.0	1	
$2Cu^+ + HS^- - H^+$ [7]	= Cu_2S	34.62	1	

1 WATEQ data base (Ball et al., 1991)
2 Bruno et al. (1992a)
3 Bruno et al. (1992b)
4 Grenthe et al. (1992)
5 Berner (1984)
6 Ion diffusivities from Wehrli (personal comm.) and assumed factor of 100 decrease for compacted clay
7 Only used in sensitivity analysis (see text)

assumed in the intermediate compartment representing the copper-bentonite boundary. The possibility of Cu(I) and Cu_2S controlling the corrosion process will be evaluated in the subsequent sensitivity analysis.

Slow processes: These are conveniently separated into chemical and transport-related processes, as outlined in section 3.2.2. The slow chemical process considered involves copper corrosion whose kinetics under anoxic conditions are not known (Leidheiser, 1971; Grauer, 1984). From thermodynamic considerations it can be inferred that the overall corrosion process involves oxidation of Cu(0) and precipitation of Cu_xS (here CuS assumed). From the former constraint it follows that oxidants or electron acceptors in the clay medium[1] play an active role in the oxidation process. The possible oxidants in the anoxic porewater are SO_4^{2-}, Fe(III), and H_2O. Reduction of sulphate is limited by microbial activity since inorganic reduction is extremely slow (KBS-3; Grauer, 1991). Microbial activity in turn is thought to be limited by the low pore space of the clay. However, there exists a certain possibility of bacterial nesting at the copper surface (Werme, personal comm.). The evaluation of this factor necessitates further data and will not be included in this work. This leaves two possibilities in terms of reaction partners for the corrosion process:

$$Cu(0) + 2Fe^{3+} + HS^- \rightarrow CuS(s) + 2Fe^{2+} + H^+ \quad (10)$$

$$Cu(0) + HS^- + H^+ \rightarrow CuS(s) + H_2(g) \quad (11)$$

It is reasonable to expect that the process described by Eq. (10) is limited by the availability of Fe(III) in the porewater which is controlled by the release of ferric oxide. The availability of Fe(III) in the corrosion process is further constrained by the diffusion of soluble Fe(III) to the copper surface. Assuming a diffusion-limited process with regard to soluble Fe(III), the corrosion rate, R_{corr}, described by Eq. (10), can be approximated by a first-order rate expression:

$$R_{corr} = k_{corr}[Fe(III)]_t \quad (12)$$

where k_{corr} is the pseudo first-order corrosion rate [dm s^{-1}] and $[Fe(III)]_t$ is the concentration of total dissolved Fe(III) [mol dm^{-3}]. Taking into account the average diffusivity of Fe(III) species in the clay porewater and the Fe(III) concentration from $Fe(OH)_3$ equilibrium using the MINEQL code (EIR version; Schweingruber, 1982), a rough upper estimate of the corrosion rate constant, $k_{corr} = 2.4 \cdot 10^{-7}$ dm s^{-1} is obtained.

The process described by Eq. (11) involves the reduction of water at the copper surface. Although experimental evidence for this process is lacking (The Swedish Corrosion Institute, 1983) it has been previously considered in the long-term safety assessment of canister corrosion (e.g.,

[1] this statement neglects the contribution of radiolysis which is usually regarded as minor factor

Neretnieks, 1983; Werme et al., 1992) in order to obtain an upper estimate of corrosion rates under the assumption that HS^- diffusion is the rate-limiting step. Here, we take the corrosion process involving iron and sulphide as reaction partners (Eq. (10)) as reference case. This choice is qualitatively supported by geological information on copper sulphide formation under supergene conditions which appears to be closely coupled to the iron cycle (Marcos, 1989). The less likely corrosion process, described by Eq. (11) will be considered under the condition of a HS^- diffusion-limited corrosion, in order of have an upper limit for the corrosion process.

Diffusion of components is treated as a series of slow processes of dissolved species between adjacent compartments as outlined for the general case in section 3.2.2. Here, we illustrate this concept by taking the example of the diffusive flux of Cu(II). As depicted in Fig. 2 mass transfer is considered to occur between the centre ("reaction box") and the two boundary compartments, the bentonite box (ben) and the canister box (can). The overall diffusive flux of component Cu(II) can thus be separated into four single fluxes in and out of "ben" and "can": J(ben,in), J(ben,out), J(can,in), J(can,out). Furthermore, the Cu(II) flux is composed by the sum of fluxes of proper species: Cu^{2+}, $Cu(OH)^+$, $Cu(OH)_2$, $Cu(OH)_3^-$, $CuCO_3(aq)$, $Cu(CO_3)_2^{2-}$, and $CuHCO_3^+$. According to Fick's law, the flux of a species, such as Cu^{2+}, $J_{Cu^{2+}}$ is:

$$J_{Cu^{2+}} = \frac{D}{\Delta x} C_0 - \frac{D}{\Delta x} C \qquad (13)$$

where D is the diffusion coefficient [$dm^2\ s^{-1}$], Δx is the diffusion distance [dm], C_0 is the Cu^{2+} conc. in the boundary compartment, ben or can, and C the Cu^{2+} steady-state concentration of the centre compartment. The diffusion coefficients of the dissolved species in the compacted bentonite medium are given in Table 1. They are estimated from diffusivities in water (Li and Gregory, 1974; Applin and Lasaga, 1984; Wehrli, personal comm.), and assuming a constant relative decrease of a factor of 100 (cf. Neretnieks and Skagius, 1978). The diffusion length, for the reference case, is taken to be 0.01 dm which appears to be a reasonable estimate for diffuse boundary layers in sedimentary systems (Furrer and Wehrli, 1992; Billen, 1982). Applying the relationship given in Eq. (13) to all the Cu(II) species and taking the sum, the flux of Cu(II) in and out of the boundary compartments is obtained. The last process to consider is the outflow which is imposed by the flow velocity and is considered in the model as perpendicular to the diffusive flux, thus parallel to the copper-bentonite boundary. In the compacted clay flow is very slow, of the order of 10^{-10} dm s^{-1}. A summary of the slow processes with the rate equations is given in Table 2, the corresponding parameters in Table 3.

Table 2 Stoichiometry of slow processes and rate equations under anoxic conditions

Process	Rate equation
1) Oxidation of Cu by Fe(III).[a] $Cu(0) + 2Fe^{3+} \rightarrow Cu^{2+} + 2Fe^{2+}$	$R_{Fe3} = k_{Fe3}\,[Fe(III)]_t$
2 Oxidation of Cu by H_2O.[a,b] $Cu(0) + 2H^{+} \rightarrow Cu^{2+} + H_2(g)$	$R_{H2O} = d_{f,HS}\,[HS^-] - d_{b,HS,ben}$
3) Diffusion in and out of bentonite-box (ben)[c] $Flux_{in}$ - $Flux_{out}$, all species	$R_{diff,ben} = d_{f,i}\,C_i - d_{b,i,ben}$
4) Diffusion in and out of copper-box (can)[c] $Flux_{in}$ - $Flux_{out}$, all species	$R_{diff,can} = d_{f,i}\,C_i - d_{b,i,can}$
5) Outflow.[d] $Flux_{out}$, all species	$R_{out} = v_{out}\,C_i$

[a] Corrosion process is separated in slow process (oxidation) and fast process (precipitation of CuS).
[b] $d_{f,HS} = D_{HS}/\Delta x$ where D_{HS} is diffusivity of HS^- in compacted bentonite and Δx is diffusion. distance; $d_{b,HS,ben} = (D_{HS}/\Delta x)*C_{HS,ben}$ where $C_{HS,ben}$ is fixed $[HS^-]$ in bentonite box.
[c] $d_{f,i} = D_i/\Delta x$ where i refers to species i; $d_{b,i,ben} = (D_i/\Delta x)*C_{i,ben}$, C_i is conc. (M) in the intermediate reaction box of any species i.
[d] v_{out} is the flow velocity.

Table 3 Value of parameters in rate equations used for reference case under anoxic conditions.

Parameter		Value	Units
1	k_{Fe3}	$2.4 \cdot 10^{-7}$	dm s^{-1}
2[a]	$d_{f,HS}$	$1.2 \cdot 10^{-7}$	dm s^{-1}
	$d_{b,HS,ben}$	$1.2 \cdot 10^{-13}$	mole dm^{-2} s^{-1}
3[a]	$d_{f,i}$	$0.2 - 6.2 \cdot 10^{-7}$	dm s^{-1}
	$d_{b,i,ben}$	variable	mole dm^{-2} s^{-1}
4[a]	$d_{b,i,can}$	variable	mole dm^{-2} s^{-1}
5	v_{out}	$1.00 \cdot 10^{-10}$	dm s^{-1}
Δx_1, Δx_2		0.01	dm

[a] D_i in Table 1.

4.1.2 Results

Fluxes:

The results for the case (reference case) in which corrosion is limited by the availability of the oxidant Fe(III) are illustrated in Fig. 3A. This shows the relationships of the fluxes of Cu and HS arising from the different processes. It indicates that a flux of $5.0 \cdot 10^{-8}$ mole Cu dm^{-2} yr^{-1} is generated via corrosion (or oxidation) and precipitated to insoluble copper sulphide, shown as negative flux. Thus, the model seperates the overall corrosion process, as given by Eq. (10), into an oxidation and a precipitation step. An inspection of the HS^- fluxes reveals that the diffusive flux from the bentonite compartment (diff. ben.) is high compared to the one consumed by copper sulphide precipitation. This imposes a constant high activity level of HS^- at the near-by of the copper surface and thus imposing a low copper removal rate. The flux induced by copper sulphide precipitation is readily converted to a uniform corrosion rate by taking into account the density of CuS and metallic Cu respectively. This yields a corrosion rate of $5.1 \cdot 10^{-8}$ mm/yr.

Fig. 3B illustrates the case in which corrosion is limited by HS^- diffusion, as described by Eq. (11). The flux of Cu arising from the corrosion process is significantly enhanced with regard to the previous case. Thus, the rate of copper sulphide precipitation is about $3.8 \cdot 10^{-6}$ mole Cu dm^{-2} yr^{-1}. The presentation of the sulphide fluxes (Fig. 3B) further illustrates the corrosion process. The flux of HS diffusing from the bentonite compartment to the copper compartment is almost entirely consumed by the precipitation reaction. The calculated corrosion of the canister amounts to $3.9 \cdot 10^{-6}$ mm/yr.

Sensitivity analysis:

Here we discuss the influence of the relevant physical and chemical parameters on the copper corrosion process. The results are illustrated in Figs. 4A and 4b in which the corrosion rate as a function of the relative change with regard to the reference case (as discussed above) is shown. In addition, the limiting case of HS^- diffusion controlling the corrosion process is given (dashed horizontal line in Fig. 4).

Fe(III): The amount of dissolved Fe(III) in the bentonite has a strong influence on the Cu corrosion rates. Fe(III) is released mainly by impurities of ferric oxide which show a range in solubility of several orders of magnitude. For the reference case a high solubility constant, as given for ferrihydrit (Langmuir, 1969) with logK = 4.9 (Eq. (7)) has been selected. A decrease in the solubility results in a linear decrease of the corrosion rate (Fig. 4A). An assumed increase of soluble Fe(III) by a factor of ten with regard to the reference case results in an equally high increase of corrosion rates. Higher amounts of dissolved Fe(III) in the bentonite are highly unlikely from a geochemical point of view and therefore are not presented in the sensibility plot.

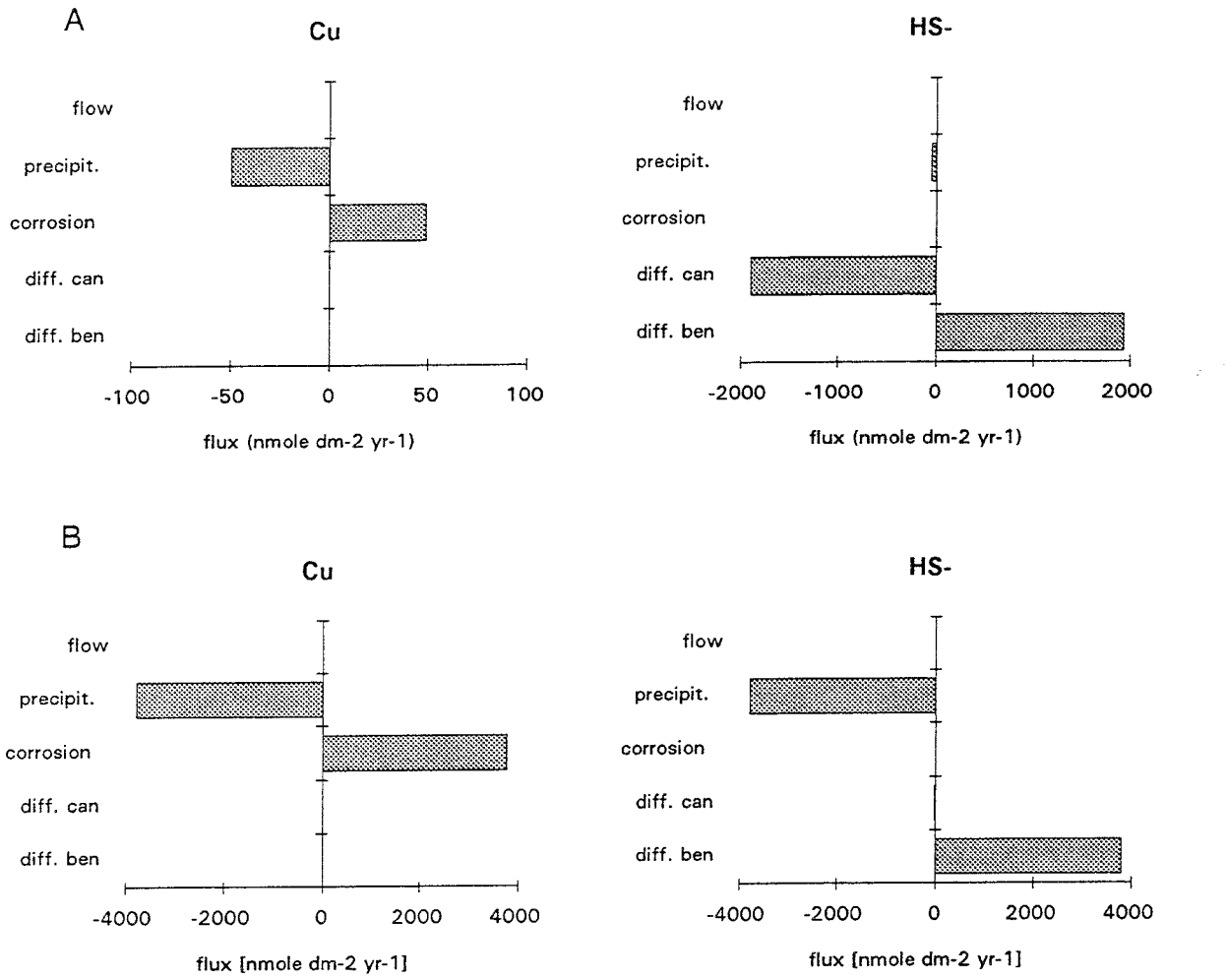

Fig. 3 Fluxes for Cu and HS^- derived from modelling results for anoxic case. "diff. can" and "diff. ben." refer to the diffusive flux into (+) or out of (-) canister and bentonite compartment, respectively. A: reference case (corrosion controlled by diffusion of reactant Fe(III)). B: limiting case of HS^--diffusion control.

pH: Proton activity in the clay medium also significantly affects release of Cu (Fig. 4A). The modelling results indicate that an increase of H^+ results in a decrease of corrosion rates down to a pH value of about 8. At further increase of H^+ a gradual increase is noted. This behaviour is explained by the speciation of Fe(III) in equilibrium with ferric oxide. Thus, at very high pH (> 9) a strong increase in corrosion rates results from the predominance of the $Fe(OH)_4^-$ species under these pH conditions. Alkalinity changes are directly related to pH changes and therefore affect rates in a similar way.

HS⁻: Taking the case of Fe(III) as oxidant, increase in the HS^- flux has no effect on corrosion Fig. 4A). Moreover, in the reference case, a rather high concentration of dissolved sulphide of 10^{-6} M imposed by FeS (freshly precipitated) is assumed in the bentonite porewater. Lowering HS^- fluxes also has a very small effect on corrosion rates in that it leads to a very slight increase of dissolved Cu(II) concentrations which are constrained by copper sulphide solubility.

Cu(I): The effect of oxidation of metal copper to Cu(I) instead of Cu(II) on the corrosion rate has also been assessed. Although Cu(I) sulphide has been calculated to be slightly less soluble than Cu(II) sulphide in the thermodynamic analysis, this may not necessarily be the case at high chloride levels, since Cu(I) forms fairly strong complexes with Cl^- (Table 1). Cl^- levels in the bentonite are expected to be relatively high, in the range of 10^{-3} to 10^{-2} M (Wanner et al., 1992) depending on the composition of the surrounding groundwater. Model calculations showed that the Cu solubility is increased by a maximum factor of 30 at highest Cl^- levels with regard to the reference case. However, the maximum total dissolved Cu concentration is still very low ($\approx 5 \cdot 10^{-15}$ M). Thus the resulting corrosion rate predicted by the model is not noteably changed with regard to the reference case.

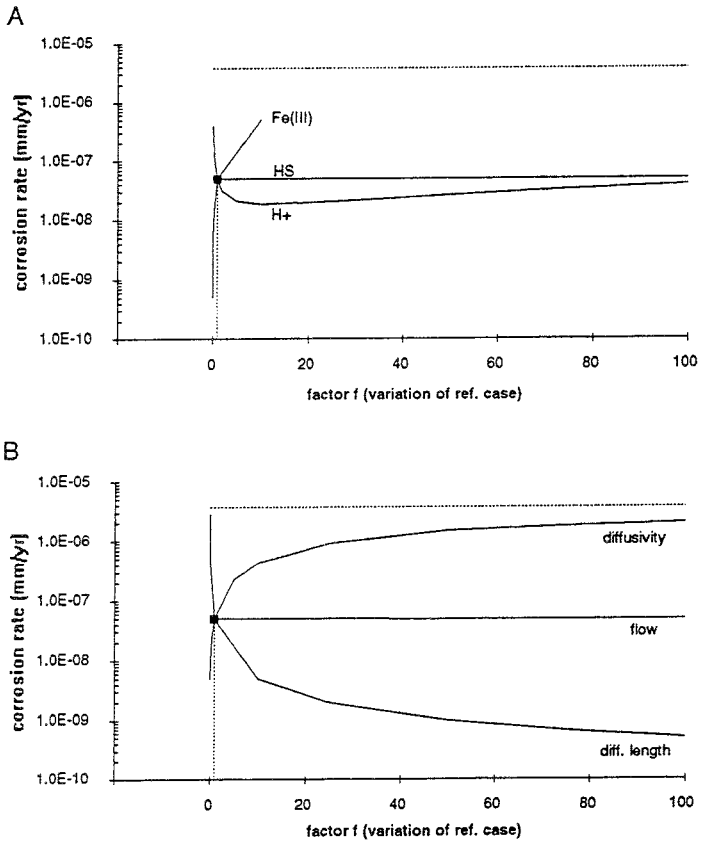

Fig. 4 Summary of sensitivity analysis showing effect of important model parameters on corrosion rate. X-axis gives variation factor f with respect to reference case (f = 1), shown as filled square. Dashed horizontal line shows result obtained for case of HS^- diffusion limitation. A: chemical parameters; B: physical parameters.

Diffusion coefficients: The diffusivity of dissolved compounds in the compacted bentonite significantly influences the corrosion process (Fig. 4B). The range of uncertainites for pore diffusivities is estimated to be a factor of about ten (Brandberg and Skagius, 1991). A ten-fold increase of the diffusion coefficients results in an eight-fold increase of corrosion rates. Decreasing the diffusivities by a factor of ten leads to an equal relative decrease in corrosion rates.

Diffusion length: Decreasing the diffusion length between the bentonite medium and the copper surface (dx_1) results in an increase of copper release (Fig. 4B). Thus, the model results indicate that a diffusion distance of 0.01 mm would lead to a corrosion rate of $3 \cdot 10^{-6}$ mm/yr. This is still below the rate derived under the assumption of rate control by HS^- diffusion. On the other hand, increase in the diffusion length leads to significantly lower corrosion rates.

Flow: As mentionned above, the model also offers the possibility to evaluate the effect of flow along the boundary of the canister surface. Fig. 4B illustrates that the corrosion is not affected even by significant variations of the flow velocity.

Summary: Fe(III) availability, pH, and diffusion properties are the main factors which exert a significant effect on corrosion within the modelling framework. Since the range of Fe(III) and pH are constrained by the geochemical conditions expected in the bentonite, it is mainly the uncertainty with regard to the diffusion properties which imposes the uncertainty of the model predictions. The sensitivity calculations indicate that the obtained range of corrosion rates is always below the one derived for HS^- diffusion limitation. From the estimated uncertainties on diffusion properties, a factor of about ten in uncertainty with reagard to the reference case appears reasonable.

4.2 Oxic corrosion of Cu

4.2.1 Boundary conditions

The boundary conditions are very similar to the ones evaluated for the anoxic case, except for the redox potential. Again we first perform an initial estimate of the geochemical variables used in the model by defining a reference case and then perform a subsequent sensitivity analysis thereof.

Fast processes: Interaction between the components H^+, CO_3^{2-}, Ca^{2+}, Fe^{2+}, Fe^{3+}, O_2, plus Cu^{2+} within the solution and with the solid matrix are modelled. Copper(II) in the presence of O_2 is limited by the solubility of copper hydroxy carbonate (malachite, cf. section 2):

$$Cu_2CO_3(OH)_2(s) + 2H^+ = 2Cu^{2+} + CO_3^{2-} + 2H_2O \qquad (14)$$

which shows rather high solubility (logK = -4.0). Because of the high alkalinity and pH expected in the bentonite porewater (Wanner et al., 1992), the activity of Cu^{2+} is fixed. A speciation calculation

with MINEQL shows Cu(II) equilibrium concentration of $1.9 \cdot 10^{-6}$ M, with the carbonate complexes $CuCO_3(aq)$ and $Cu(CO_3)_2^{2-}$ as predominant species. This indicates that the expected Cu(II) diffusive fluxes to the limiting bentonite and canister compartments are much higher compared to the anoxic case where extremely low Cu(II) concentrations are expected. Therefore, these thermodynamic constraints already suggest significantly higher corrosion rates under oxic conditions. Further solid equilibria reactions include calcite and ferric oxide (Eqs. (6) and (7). A summary of all fast processes and corresponding equilibrium constants is given in Table 4.

Table 4 Stoichiometry of fast processes with equilibrium constant and diffusivities (oxic case)

Reaction		logK	source	[5]diffusivity $1 \cdot 10^{-7} * cm^2 s^{-1}$
Aqueous phase:				
H^+	$= H^+$	0		6.27
CO_3^{2-}	$= CO_3^{2-}$	0		0.50
Cu^{2+}	$= Cu^{2+}$	0		0.41
Ca^{2+}	$= Ca^{2+}$	0		0.42
Fe^{3+}	$= Fe^{3+}$	0		0.20
O_2	$= O_2$	0		1.26
$H_2O - H^+$	$= OH^-$	-14.00	1	3.17
$CO_3^{2-} + 2H^+$	$= H_2CO_3$	16.68	1	1.20
$CO_3^{2-} + H^+$	$= HCO_3^-$	10.33	1	0.71
$HS^- + H^+$	$= H_2S$	7.02	1	1.56
$Cu^{2+} - H^+$	$= Cu(OH)^+$	-8.00	1	1.00
$Cu^{2+} - 2H^+$	$= Cu(OH)_2$	-16.20	1	1.00
$Cu^{2+} - 3H^+$	$= Cu(OH)_3^-$	-26.30	1	1.00
$Cu^{2+} + CO_3^{2-}$	$= CuCO_3$	6.77	1	0.32
$Cu^{2+} + 2CO_3^{2-}$	$= Cu(CO_3)_2^{2-}$	10.10	1	0.32
$Cu^{2+} + CO_3^{2+} + H^+$	$= CuHCO_3^+$	14.62	1	0.45
$Ca^{2+} + CO_3^{2-}$	$= CaCO_3$	3.22	1	0.34
$Ca^{2+} + CO_3^{2-} + H^+$	$= CaHCO_3^+$	11.44	1	0.45
$Fe^{3+} - H^+$	$= Fe(OH)^{2+}$	-2.19	1	0.60
$Fe^{3+} - 2H^+$	$= Fe(OH)_2^+$	-5.67	1	1.00
$Fe^{3+} - 3H^+$	$= Fe(OH)_3$	-13.09	1	1.00
$Fe^{3+} - 4H^+$	$= Fe(OH)_4^-$	-21.60	1	1.00
$Fe^{3+} + CO_3^{2-} - H^+$	$= FeOHCO_3$	3.83	3	0.32
$Fe^{3+} + 2CO_3^{2-}$	$= Fe(CO_3)_2^+$	7.40	3	0.32
Solid phase:				
$Ca^{2+} + CO_3^{2-}$	$= CaCO_3$	8.48	1	
$Fe^{3+} + 3H_2O - 3H^+$	$= Fe(OH)_3$	0.4	4	
$2Cu^{2+} + CO_3^{2-} - 2H^+$	$= CuCO_3(OH)_2$	4.0	1	

1 WATEQ data base (Ball et al., 1991)
2 Bruno et al. (1992a)
3 Bruno et al. (1992b)
4 Grenthe et al. (1992)
5 Ion diffusivities: Wehrli (personal comm.) and assumed factor of 100 decrease for compacted clay.

Slow processes: The overall corrosion process involves transformation of Cu(0) to Cu(II) by molecular oxygen:

$$2Cu(0) + O_2 + 4H^+ \text{----> } 2Cu^{2+} + 2H_2O \qquad (15)$$

Furthermore, the activity of Cu^{2+} is fixed by the solubility of malachite (Eq. (14)) at the canister surface. As outlined above, this induces a high Cu(II) backward flux to the non-oxidized copper metal. This flux must be must be lower than the one generated by oxidation. The modelling framework allows a convenient way to constrain the overall corrosion flux (Eq. (15)) by separation into two processes: oxidation and conproportionation:

$$4Cu^+ + O_2 + 4H^+ \text{---> } 4Cu^{2+} + 2H_2O \qquad (15a)$$

and

$$2Cu^{2+} + 2Cu(0) \text{---> } 4Cu^+ \qquad (15b)$$

Thus, the flux of generated Cu(I) is half the one of generated Cu(II). The overall corrosion rate is constrained by the condition where corrosion $^1/_2$flux = backward flux. Under the assumption of steady-state and excess O_2 with regard to dissolved Cu, the corrosion rate of can then be evaluated as a function of the diffusion distance between the metal and the diffusion layer (dx_2). This is illustrated in Fig. 5 where the inverse relationship between diffusion layer thickness and corrosion rate is shown. Taking a diffusion layer thickness of 1 mm, a corrosion rate R_{corr} of $1.1 \cdot 10^{-13}$ mole Cu dm^{-2} s^{-1} is obtained, which is used for the reference case.

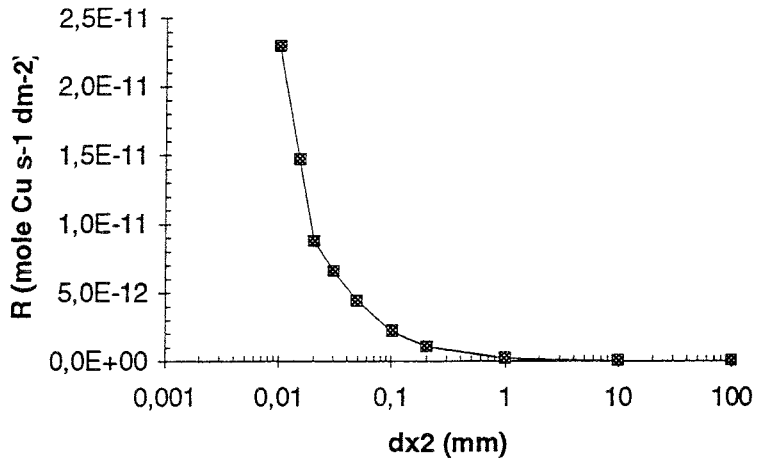

Fig. 5 Effect of diffusion length between metal surface and and intermediate box (dx_2) on corrosion rate R in mole Cu dm^{-2} s^{-1}.

Diffusion processes are treated as for the anoxic case. Diffusivities for each species are given in Table 4. A summary of slow processes and rate equations is given in Table 5 and the correponding parameters in Table 6.

Table 5 Stoichiometry of slow processes and rate equations under oxic conditions

Process	Rate equation
1) Oxidation of Cu[a] $2Cu(0) + O_2 + 4H^+ \text{----> } 2Cu^{2+} + 2H_2O$	$R_{O2} = k_{O2}$
2) Diffusion in and out of bentonite-box (ben)[b] $Flux_{in}$ - $Flux_{out}$, all species	$R_{diff,ben} = d_{f,i}\, C_i - d_{b,i,ben}$
3) Diffusion in and out of copper-box (can) $Flux_{in}$ - $Flux_{out}$, all species	$R_{diff,can} = d_{f,i}\, C_i - d_{b,i,can}$
5) Outflow.[c] $Flux_{out}$, all species	$R_{out} = v_{out}\, C_i$

[a] Corrosion process is separated in slow process (oxidation) and fast process (precipitation of $Cu_2CO_3(OH)_2$).
[b] $d_{f,i} = D_i/\Delta x$ where i refers to species i; $d_{b,i,ben} = (D_i \Delta x)*C_{i,ben}$, C_i is conc. (M) in the intermediate reaction box of any species i.
[c] v_{out} is the flow velocity.

Table 6 Value of parameters in rate equations used for reference case under oxic conditions.

Parameter		Value	Units
1	k_{O2}	$2.20 \cdot 10^{-13}$	mole dm^{-2} s^{-1}
3[a]	$d_{f,i}$	$0.2 - 6.2 \cdot 10^{-7}$	dm s^{-1}
	$d_{b,i,ben}$	variable	mole dm^{-2} s^{-1}
4[a]	$d_{b,i,cop}$	variable	mole dm^{-2} s^{-1}
5	v_{out}	$3.1 \cdot 10^{-11}$	dm s^{-1}
	Δx_1, Δx_2	0.01	dm

[a] D_i in Table 1.

4.2.2 Results

Fluxes:

Steady-state fluxes in the near-by of the canister have been calculated for the boundary conditions discussed above. Fig. 6 illustrates that the Cu fluxes are high compared to anoxic corrosion (4-300 times higher). From the constraint imposed on the overall corrosion rate where half of the flux is consumed by the internal Cu(II)-Cu(I)-Cu(0) cycling, as depicted by the diffusive flux to the canister ("diff. can"), it follows that half of generated Cu(II) is released from the canister surface. Furthermore, in the case of equal diffusive layer thickness between the two limiting compartments and the boundary layer (as assumed for the reference case), the amount of Cu removal from precipitation is minimal at steady state (Fig. 6). Thus, the remaining half of the total Cu(II) flux diffuses away from the boundary layer ("diff. ben"). This flux is $7.0 \cdot 10^{-6}$ mole Cu dm^{-2} s^{-1} which, converted to a uniform copper corrosion rate, yields $7.1 \cdot 10^{-6}$ mm/yr. Fig. 6 also shows O_2 fluxes which indicate that only a small fraction of O_2 diffusing to the canister is consumed by the corrosion process. At an assumed dissolved O_2 content of $2 \cdot 10^{-4}$ M in the bentonite compartment, which represents a very early stage of the repository (Neretnieks, 1983; Wersin et al., 1994), only 2% of the O_2 flux is removed by canister corrosion. Thus, the model suggests, that, for a large range of concentrations in the porewater of the clay, O_2 is excess with regard to dissolved Cu and therefore corrosion rates can be considered relatively constant over large range of $[O_2]$. Fluxes of carbonate remain unaffected from the corrosion process due to the high alkalinity of system.

The derived corrosion rate of $7.0 \cdot 10^{-6}$ mm/yr is in surprisingly good agreement with archeological data. In fact, Hallberg et al. (1988) estimated a corrosion depth of $1.5 \cdot 10^{-5}$ mm/yr, based on observations of a bronze cannon embedded in clay sediments. This gives support to the estimated geochemical variables in our modelling approach.

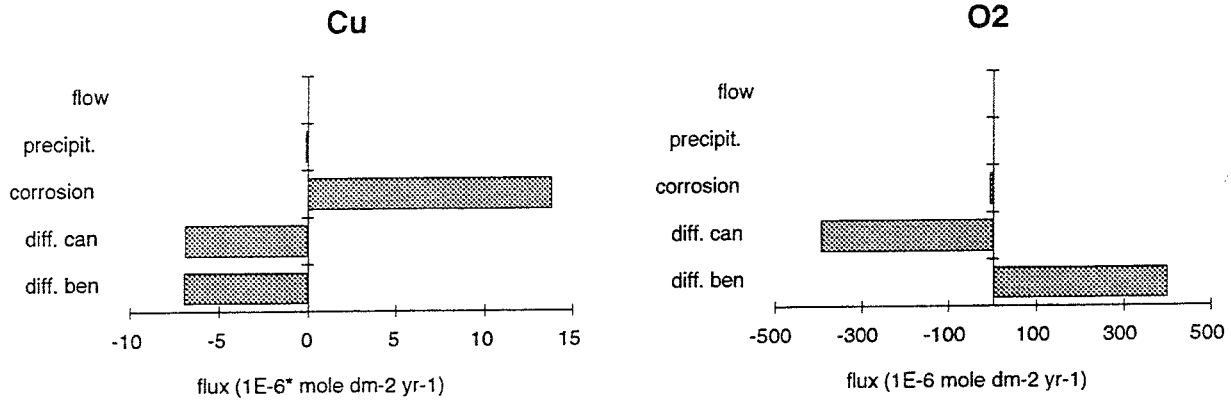

Fig. 6 Fluxes for Cu and O_2 derived from modelling results for the reference under oxic conditions. "Diff. can" and "diff. ben." refers to the diffusive flux into (+) or out of (-) canister and bentonite compartment, respectively.

Sensitivity analysis:

The sensitivity of the corrosion rate with regard to the main chemical and physical parameters is illustrated in Figs. 7A and 7B.

CO_3: The amount of total CO_3 (or alkalinity) strongly affects corrosion rates (Fig. 7A). This is due to the carbonate ligand which complexes Cu(II) and thus leads to increased solubility. However, significant increase of the alkalinity in the clay medium with regard to the reference case is not expected since experimental data (Werme (unpubl.), 1988; Snellman, 1984) indicate that the assumed alkalinity in the reference case ($8 \cdot 10^{-3}$ M) represents a relatively high concentration. Lowering of carbonate with regard to this value results in a strong decrease in dissolved Cu(II) concentrations and in the corrosion rates.

pH: Increase in proton activity (decreasing pH) in the clay medium leads to increase in corrosion rates. This arises from its effect on free carbonate which decreases simultaneously and therefore leads to higher Cu^{2+} concentrations in equilibrium with malachite and higher Cu(II) fluxes.

O_2: Fig. 7A illustrates that large variations of $[O_2]$ in the clay have no effect on corrosion rates since O_2 fluxes are in excess with regard to Cu(II) fluxes. This result simplifies time scale estimations as discussed in the following section (section 5).

Diffusion coefficients: The diffusivities of dissolved species in the compacted bentonite strongly influence corrosion. The model predicts a linear relationship between diffusion coefficients and corrosion rates (Fig. 7B). The range of uncertainites for pore diffusivities is estimated to be a factor of about ten (Brandberg and Skagius, 1991).

Diffusion length: A decrease in the imposed distance between the canister surface and the clay ($\Delta x = dx_1 + dx_2$) has a large effect on corrosion rates, in a similar way as increased diffusion coeffiecients. An increase of dx_1, however, does not alter the overall Cu(II) flux as long as the thickness of the diffusive layer and the metal surface (dx_2) remains constant (1 mm in the reference case). The effect of dx_2 on the corrosion rate has been shown in Fig. 5 , indicating an inverse relationship. From the study of diffusion profiles in lacustrine systems (Furrer and Wehrli, 1992) and marine sediments (Billen, 1982), diffusion layer thicknesses are in the range of 0.1 to 1 mm. Taking 0.1 mm for both dx_1 and dx_2 a corrosion rate of $6.9 \cdot 10^{-5}$ mm/yr is obtained.

Flow: Fig. 7B illustrates that corrosion is not affected by significant variations of the flow velocity.

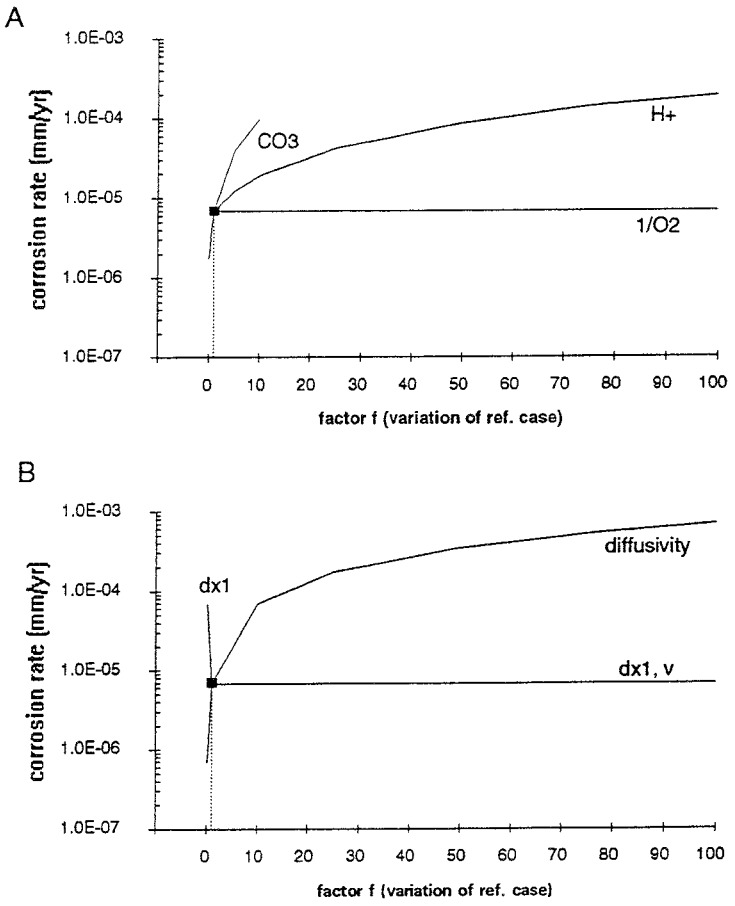

Fig. 7 Summary of sensitivity analysis showing effect of important model parameters on corrosion rate. X-axis gives variation factor f with respect to reference case (f = 1), shown as filled square. A: chemical parameters; B: physical parameters.

5 Time scales

5.1 Evolution of redox conditions in the clay

5.1.1 Concept for time scale assessment

Fig. 8 schematically summarizes the concept used for estimating time scales of canister corrosion in a repository. The redox potential, Eh, in the clay medium is the main variable controlling the corrosion process (Fig. 8A) for any given time t. Eh is expected to change with time from oxic to anoxic conditions. Thus, time scales of corrosion can be approximated by considering corrosion under both oxidizing and reducing conditions and derive realistic corrosion rates thereof (Fig. 8B). Furthermore, the evolution of Eh with time must be known. In the following the results obtained in a recent work (Wersin et al., 1994) concerning O_2 and Eh evolution are briefly outlined.

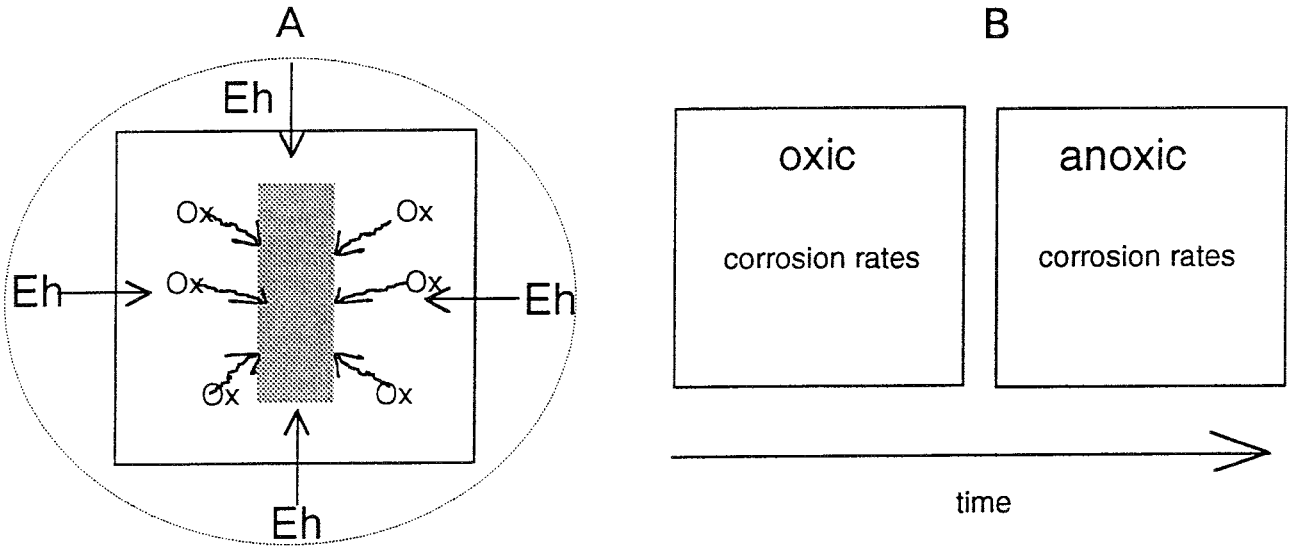

Fig. 8 The redox potential (Eh) in the clay is the main geochemical variable affecting the corrosion process in the repository (A). It determines the nature of oxidants (Ox) reacting with the canister surface. Estimation of time scales depends on corrosion rates under oxic and anoxic conditions and on the time of oxic/anoxic transition in the clay (B).

5.1.2 Time scales for Eh

O_2 in the bentonite which is entrained initially is consumed fairly rapidly via reaction with electron donors. Thus, calculations have shown that the reaction with the available pyrite impurities in the clay is much faster than diffusion towards the surrounding anoxic bedrock (Wersin et al., 1994). The time of O_2-consumption below 1% of initial value was estimated to occcur between 7 and 280 years mainly depending on the uncertainty in oxidation kinetics. The use of a geochemical model based on STEADYQL, similar to the one used here, allowed to predict the evolution of redox equilibria. These results are summarized in Fig. 9. The dashed and the solid curve show the evolution of Eh with time at fast and slow oxidation kinetics, respectively. Thus, the range between the two curves represents the uncertainty range of transition from oxic to anoxic transitions. Under oxic conditions Eh is assumed to be controlled by oxygen partial pressure which yields an Eh of 0.6-0.7 mV. These values represent an upper limit, since, in the majority of cases, observed field Eh values are considerably lower. Under anoxic conditions Eh is assumed to be controlled by the Fe^{3+}/Fe^{2+} redox couple, where Fe^{3+} activities are fixed by ferric oxide solubility. Taking an intermediate solubility constant ($\log K_{Fe(OH)_3}$ = -42.4), as deduced from redox measurements in granitic groundwaters (Grenthe et al., 1992), Eh values between -0.3 and -0.4 mV are obtained (Fig. 9). The results indicate that the transition from oxic to anoxic conditions is expected to occur beween 7 and 280 years after sealing of the repository.

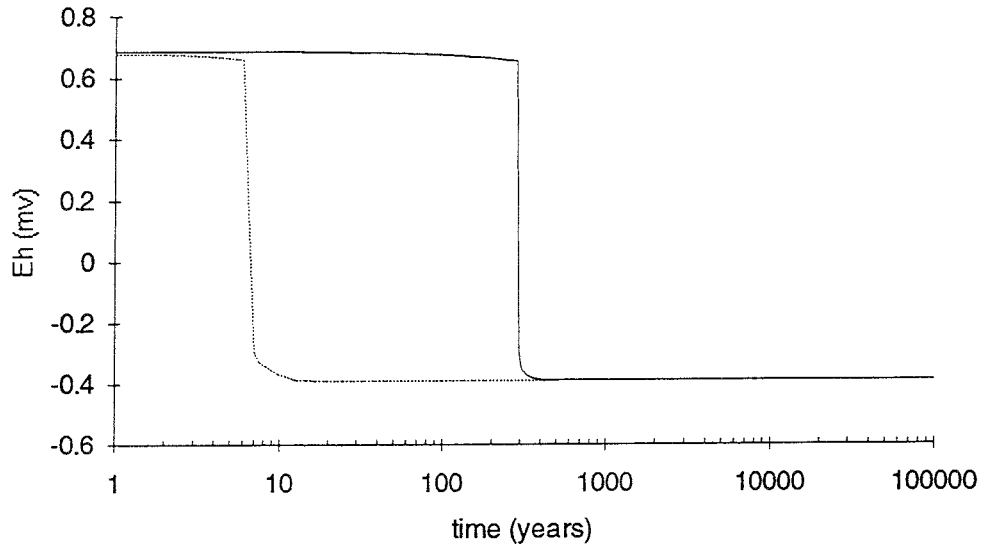

Fig. 9 Time evolution of Eh in the clay as predicted from STEADYQL calculations of Wersin et al. (1994). Dashed refers to minimum time and solid line to maximum time predicted for oxic/anoxic transition.

5.2 Synthesis of results

5.2.1 Corrosion under oxic conditions

The corrosion rates obtained from the model show good agreement with archeological data analyzed by Hallberg et al. (1988). Thus, the calculated rate for the assumed reference case agrees with the estimates of these authors within a factor of two. From the sensitivity analysis of the model, it can be inferred that the main uncertainties in predictions are related to diffusion properties of the system. Uncertainties thereof lead to an estimated uncertainty of a factor of ten with regard to the reference case.

At oxic conditions, i.e. high redox potentials, the corrosion process is expected to proceed at a constant rate in view of the high buffering capacity (high alkalinity) in the bentonite medium and because O_2 fluxes are much higher than expected Cu(II) fluxes. Once O_2 fluxes have reached levels comparable to the one of Cu(II) the system is expected to exhibit low Eh conditions (< 0 mV), which are controlled by the Fe^{2+}/Fe^{3+} redox couple (Wersin et al., 1994). The transition from oxic to anoxic conditions was estimated to occur between a time scale of 7 to 280 years which results from the uncertainty associated with O_2 consumption rates. An intermediate rate would yield 65 years for the time of transformation.

In the modelling approach a uniform corrosion rate has been implicitely assumed. However, localized corrosion of copper may lead to increase of corrosion depths. Thus, on the basis of archeological observations (Bresle et al., 1983), pitting factors of 2-5 have been suggested for safety assessment (KBS-3; SKB 91). The effect of local corrosion strongly depends on the redox potential (Grauer, 1984).

There are thus three different types of uncertainites associated with corrosion rate under oxic conditions:

- model
- time scale of oxic/anoxic transition
- pitting factor

In view of this we propose to consider a realistic and a conservative estimate of time scales.

Realistic case: The good agreement between modelling results and the independent archeological study of Hallberg et al. (1988) justifies the obtained rate of uniform corrosion of $7 \cdot 10^{-6}$ mm/yr. Furthermore, a relative high pitting factor of five is selected (KBS-3) in view the high uncertainties associated with local corrosion effects. This gives $4 \cdot 10^{-5}$ mm/yr. The time scale of corrosion under oxic conditions is taken to be 65 years. This would yield $3 \cdot 10^{-3}$ mm within this time period.

Conservative case: From the uncertainties related to the modelling results a ten-fold increase of the corrosion rate, compared to the one obtained by the reference case, is not unreasonable. Further, assuming a strong effect of local corrosion, with a very high pitting factor of 100, a rate of $7 \cdot 10^{-3}$ mm/yr results. This value is in fact very close to the upper range of corrosion depths reported for pipe-lines (~ 0.01 mm) (Leidheiser, 1971), (disregarding the pipes at very high CO_2 content and high hydraulic regimes). The upper time scale of corrosion under oxic conditions is 280 years. This would finally give a maxium estimate of corrosion depth of 2 mm during this time period.

The time scales of corrosion are summarized in Fig. 10.

5.2.2 Corrosion under anoxic conditions

Inspite of the lack of experimental data, thermodynamic, kinetic, and transport-related constraints, as elaborated in the model, allow to establish Cu fluxes in the clay medium and to derive realistic corrosion rates. The obtained rates are, as expected from the low solubility of copper sulphide, much lower compared to the ones obtained at high redox potentials. Thus, taking the interaction of the electron acceptor Fe(III) with the copper surface as diffusion-limited process with regard to Fe(III), a corrosion rate of $5 \cdot 10^{-8}$ mm/yr is calculated. From the sensitivity analysis performed on the model, it can be inferred, that the uncertainties within the modelling framework are not very large, giving rise to a factor of about ten with regard to the above value. On the other hand, taking

diffusion of HS^- to the canister surface as controlling the corrosion rate, yields an upper rate of $4 \cdot 10^{-6}$ mm/yr.

Low redox potentials are expected to occur in th near field after time of maximum 280 years (Fig. 9). Therefore, correponding corrosion rates will predominate in the life-time of a canister. At low redox potentials, the effect of local corrosion is expected to be small. Furthermore, the homomogeneity of the surrounding clay medium and its physical properties suggest a homogeneous corrosion process (Grauer, 1984). Therefore, pitting corrosion with factors higher than 2-5 do not appear to be probable.

In summary, the uncertainties associated with corrosion rates under anoxic conditions appear to be rather low in spite of the lack of experimental and archeological information. Again we suggest to consider a realistic and conservative case.

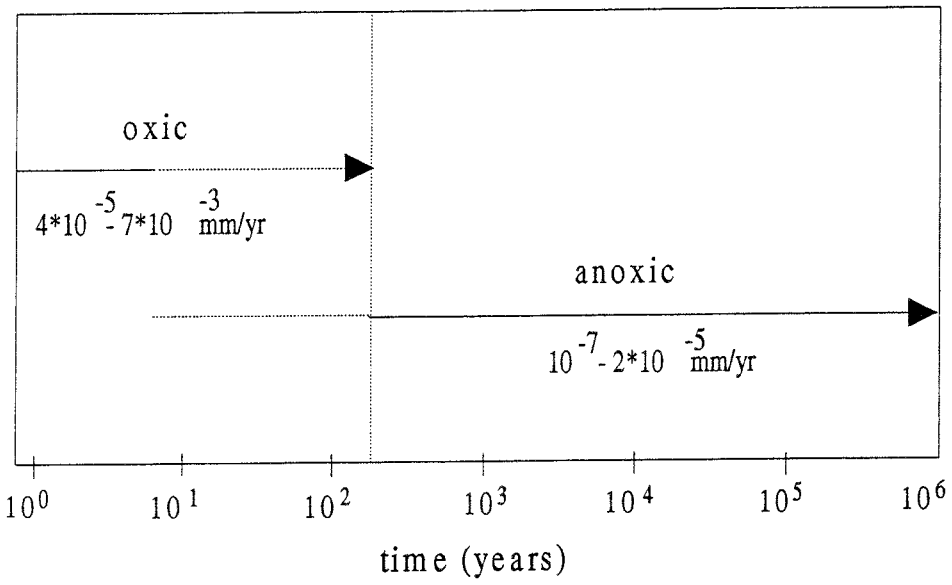

Fig. 10 Estimated time scales for copper canister corrosion depths. Dashed horizontal gives range of uncertainty for time of oxic/anoxic transition in the clay. Note logarithmic scale for time axis.

Realistic case: A corrosion rate of $5 \cdot 10^{-8}$ mm/yr (reference case in the modelling approach) and a pitting factor of two are selected, thus giving rise to a corrosion depth of 10^{-7} mm/yr.

Conservative case: An upper rate of $4 \cdot 10^{-6}$ mm/yr results under the assumption of HS^- diffusion, as rate limiting step. Further a pitting factor of five is selected. This results in maximum corrosion depth of $2 \cdot 10^{-5}$ mm/yr.

The obtained rates are visualized in Fig. 10.

5.2.3 Summary

Fig. 11 summarizes corrosion depths of a copper canister as a function of time. On a semi-logarithmic and double-logarithmic plot, respectively (A and B). Fig. 11A visualizes absolute increase in depth with time. Thus, a corrosion depth of merely 0.1 mm in 1 mio years is predicted for the realistic case whereas 22 mm are predicted for the conservative case. In any case the predicted corrosion depths are much lower than the canister thickness (50 mm). In Fig. 11B the change in corrosion behaviour as result depletion of O_2 and concomittant lowering of Eh is displayed.

5.3 Further uncertainties

Further uncertainties arise which have not been explicitely considered in the modelling. One factor regards the influence of increased temperature since the model is based on data valid for 25°C. There is clearly some lack in reliable data although some information in terms of equilibrium constants and diffusivities at higher T could be obtained. However, there is one argument regarding oxygen consumption which can be readily brought into play. In fact, experimental data of Nicholson et al. (1988) have shown that pyrite oxidation increases by a factor of 10 beween 25 and 60°C. This suggests that O_2 is consumed at a significantly higher rate at higher T which would decrease the time of oxic to anoxic transition in a repository. Thus, higher T would further limit high corrosion depths although slightly higher Cu metal weathering is expected.

The possibility of bacterial nesting on the canister surface has also been invoked (Werme, pers. comm.). Although this process does seem to be very likely (cf. section 4.1.1), a closer look to this possible effect by a bibliographic review may yield some more quantitative insight.

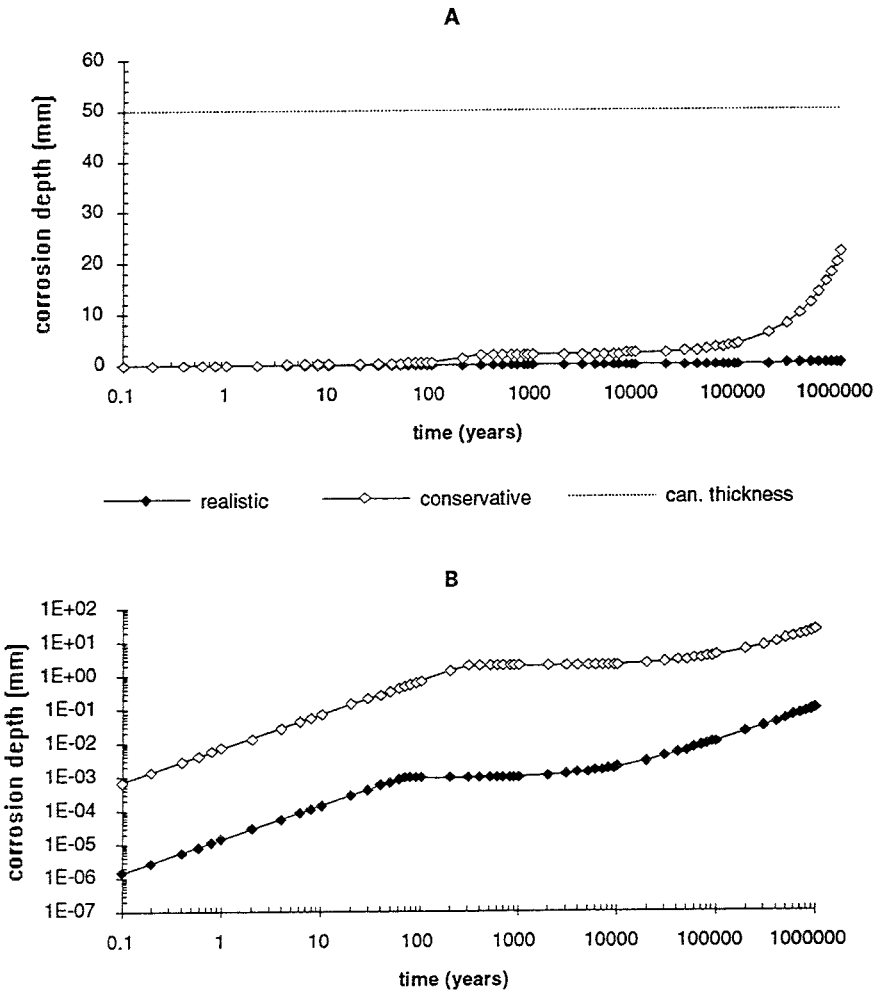

Fig. 11 Evolution of corrosion with time according to conservative (open symbols) and realistic scenario (filled symbols). Dashed line shows canister thickness. A: semi-logarithmic plot; B: double-logarithmic plot.

6 Conclusions

A new modelling approach for canister corrosion in a HLW repository has been presented. This model is based on a recently developed extension of the STEADYQL code and includes diffusional transport in addition to flow, equilibrium reactions and kinetic processes at the bentonite- canister interface. Geochemical boundary conditions are formulated for an anoxic and oxic case and corrosion rates are derived. A sensitivity analysis which evaluates the effect of uncertainties within the geochemical boundary conditions, indicates that the main uncertainties arise from the diffusional properties in the clay.

Assessment of time scales includes recent calculations on the time range of oxic/anoxic transition in the bentonite medium (Wersin et al., 1994) and pitting corrosion. This indicates realistic corrosion depths of 10^{-7} and $4 \cdot 10^{-5}$ mm/yr, respectively for anoxic and oxic conditions. Conservative estimates on corrosion depths give rise to $2 \cdot 10^{-5}$ and $7 \cdot 10^{-3}$ mm/yr, respectively. From these conservative estimates a corrosion depth of maximum 22 mm in 1 mio years is calculated which compares to the envisioned canister thickness of 50 mm.

Chemical corrosion of copper canisters does not appear to constitute a problem for repository safety although other factors such as increased temperature have not been explicitely included in the model. It is suggested that the possible effect of bacteria on corrosion is further studied as it may possibly enhance locally the described redox processes.

7 Acknowledgements

We would like to thank Dr. Gerhard Furrer (ETH Zürich) and Dr. Lars Werme (SKB) for helpful comments and Dr. Bernhard Wehrli (ETH Zürich) for providing valuable diffusion data.

8 References

Applin K.R., Lasaga A.C. (1984) The determination of SO_4^{2-}, $NaSO_4^-$, and $MgSO_4^0$ trace diffusion coefficients and the application to diagenetic flux calculations. Geochim. Cosmochim. Acta 48, 2151-2162.

Ball J.W., Nordstrom D.K., Jenne E.A. (1991) Additional and revised thermodynamical data and computer code for WATEQ2- a computerized chemical model for trace and major element speciation and mineral equilibria of natural waters. U.S. Geol. Surv. Supply Inv. 78-116.

Berner R.A. (1971). Principles of sedimentology. McGraw Hill.

Berner R.A. (1984). Sedimentary pyrite formation: An update. Geochim. Cosmochim. Acta 48, 605-615.

Billen G. (1982) Modelling the processes of organic matter degradation and nutrients recycling in sedimentary systems. In: Sediment Microbiology (eds. D.B. Nedwell and C.M. Brown). Academic Press, pp. 15-52.

Brandberg F., Skagius K. (1991). Porosity, sorption, and diffusivity data compiled for the SKB 91 study. SKB Technical Report 91-16.

Bresle A., Saers J., Arrhenius B. (1983). Studies in pitting corrosion on archaeological bronzes. SKB Technical Report 83-05.

Bruno J., Wersin P., Stumm W. (1992a). On the influence of carbonate in mineral dissolution: II. The solubility of $FeCO_3$(s) at 25°C and 1 atm total pressure. Geochim. Cosmochim. Acta 56, 1149-1155.

Bruno J., Stumm W., Wersin P., Brandberg F. (1992b) On the influence of carbonate on mineral dissolution. Part I. Thermodynamics and kinetics of hematite dissolution in bicarbonate solutions at T = 25°C. Geochim. Cosmochim. Acta 56, 1139-1148.

Furrer G., Westall J., Sollins P. (1989) The study of soil chemistry through quasi-steady-state models: I. Mathematical definition of model. Geochim. Cosmochim. Acta 53, 595-601.

Furrer G., Westall J., Sollins P. (1990). The study of soil chemistry through quasi-steady-state models: II. Acidity of soil solutions. Geochim. Cosmochim. Acta 54, 2363-2374.

Furrer G., Wehrli B. (1992). Biogeochemical processes at the sediment-water interface: Measurements and modeling. Appl. Geochem. Suppl. No. 2, 117-119.

Grauer R. (1984). Behältermaterialien für die Endlagerung hochradioaktiver Abfälle: Korrosionschemische Aspekte. EIR - Bericht Nr. 523.

Grauer R. (1991). The reducibility of sulphuric acid and sulphate in aqueous solution. PSI-Bericht Nr. 109.

Grenthe I., Stumm W., Laaksoharju M., Nilsson A.-C., Wikberg P. (1992). Redox potentials and redox reactions in deep groundwater systems. Chem. Geol. 98, 131-150.

Hallberg R.O., Östlund P., Wadsten T. (1988). Inferences from a corrosion study of a bronze cannon, applied to high level nuclear waste disposal. Appl. Geochem. 3, 273-280.

KBS-3. Final storage of spent nuclear fuel (1983). Swedish Nuclear Fuel Supply Co/Division KBS, Stockholm.

Langmuir D. (1969) The Gibbs free energies of substances in the system $Fe-O_2-H_2O-CO_2$ at 25°C. USGS Prof. Paper 650-B, 180-183.

Leidheiser H. (1971). The corrosion of copper, tin and their alloys. J. Wiley & Sons.

Li Y.H., Gregory S. (1974) Diffusion of ions in sea water and in deep-sea sediments. Geochim. Cosmochim. Acta 38, 703-714.

Marcos N. (1989). Native copper as a natural analogue for copper canisters. Report YJT-89-18. Espoo, Finland.

Neretnieks I. (1983) Approximate calculation of what happens with oxygen that is entrapped in the repository at the time of its closure. In Corrosion resistance of a copper canister for spent nuclear fuel. The Swedish Corrosion Research Institute and its reference group. Appendix 4, pp. 39-45.

Neretnieks I., Skagius C. (1978). Diffusivitetsmätningar av metan och väte i våt lera. KBS Technical Report 86.

Nicholson R.V., Gilham R.W., Reardon E.J. (1988). Pyrite oxidation in carbonate-buffered solution: 1. Experimental kinetics. Geochim. Cosmochim. Acta 52, 1077-1085.

Schweingruber M. (1982) User's guide for extended MINEQL (EIR version)- standard routine package, EIR internal report TM-45-82-38, Würenlingen, Switzerland.

SKB 91. Final disposal of spent fuel. Importance of the bedrock for safety (1992). Swedish Nuclear Fuel Supply Co/Division KBS, Stockholm.

Snellman M. (1984) Chemical conditions in a repository for spent fuel. YJT 84-08. Espoo, Finland.

Strömberg B., Banwart S.(1994) Kinetic modelling of geochemical processes at the Aitik mining waste rock site in northern Sweden. Appl. Geochem. (in press).

The Swedish Corrosion Research Institute and its Reference Group (1983). Copper as canister material for unreprocessed nuclear waste - evaluation with respect to corrosion. SKB Technical Report 83-24.

Wanner H. (1986) Modelling interaction of deep groundwater with bentonite and radionuclide speciation. Nagra Tecnical Report NTB 86-21, Baden, Switzerland.

Wanner H., Wersin P., Sierro N. (1992). Thermodynamic modelling of bentonite-groundwater interaction and implications for near field chemistry in a repository for spent fuel. SKB Technical Report 92-37.

Werme L., Sellin P., Kjellbert N. (1992). Copper canisters for nuclear high level waste disposal. Corrosion aspects. SKB Technical Report 92-26.

Werme L. (1988) (unpubl.). Cited in Wanner et al. (1992).

Wersin P., Bruno J., Spahiu K. (1993) Kinetic modelling of bentonite - canister interaction. Implications for Cu, Fe, and Pb corrosion in a repository for spent nuclear fuel. SKB Technical Report 93-16.

Wersin P., Spahiu K., Bruno J. (1994) Time evolution of dissolved oxygen and redox conditions in a HLW respository. SKB Technical Report 94-02.

List of SKB reports

Annual Reports

1977-78
TR 121
KBS Technical Reports 1 – 120
Summaries
Stockholm, May 1979

1979
TR 79-28
The KBS Annual Report 1979
KBS Technical Reports 79-01 – 79-27
Summaries
Stockholm, March 1980

1980
TR 80-26
The KBS Annual Report 1980
KBS Technical Reports 80-01 – 80-25
Summaries
Stockholm, March 1981

1981
TR 81-17
The KBS Annual Report 1981
KBS Technical Reports 81-01 – 81-16
Summaries
Stockholm, April 1982

1982
TR 82-28
The KBS Annual Report 1982
KBS Technical Reports 82-01 – 82-27
Summaries
Stockholm, July 1983

1983
TR 83-77
The KBS Annual Report 1983
KBS Technical Reports 83-01 – 83-76
Summaries
Stockholm, June 1984

1984
TR 85-01
Annual Research and Development Report 1984
Including Summaries of Technical Reports Issued during 1984. (Technical Reports 84-01 – 84-19)
Stockholm, June 1985

1985
TR 85-20
Annual Research and Development Report 1985
Including Summaries of Technical Reports Issued during 1985. (Technical Reports 85-01 – 85-19)
Stockholm, May 1986

1986
TR 86-31
SKB Annual Report 1986
Including Summaries of Technical Reports Issued during 1986
Stockholm, May 1987

1987
TR 87-33
SKB Annual Report 1987
Including Summaries of Technical Reports Issued during 1987
Stockholm, May 1988

1988
TR 88-32
SKB Annual Report 1988
Including Summaries of Technical Reports Issued during 1988
Stockholm, May 1989

1989
TR 89-40
SKB Annual Report 1989
Including Summaries of Technical Reports Issued during 1989
Stockholm, May 1990

1990
TR 90-46
SKB Annual Report 1990
Including Summaries of Technical Reports Issued during 1990
Stockholm, May 1991

1991
TR 91-64
SKB Annual Report 1991
Including Summaries of Technical Reports Issued during 1991
Stockholm, April 1992

1992
TR 92-46
SKB Annual Report 1992
Including Summaries of Technical Reports Issued during 1992
Stockholm, May 1993

1993
TR 93-34
SKB Annual Report 1993
Including Summaries of Technical Reports Issued during 1993
Stockholm, May 1994

Technical Reports
List of SKB Technical Reports 1994

TR 94-01
Anaerobic oxidation of carbon steel in granitic groundwaters: A review of the relevant literature
N Platts, D J Blackwood, C C Naish
AEA Technology, UK
February 1994

TR 94-02
Time evolution of dissolved oxygen and redox conditions in a HLW repository
Paul Wersin, Kastriot Spahiu, Jordi Bruno
MBT Technología Ambiental, Cerdanyola, Spain
February 1994

TR 94-03
Reassessment of seismic reflection data from the Finnsjön study site and prospectives for future surveys
Calin Cosma[1], Christopher Juhlin[2], Olle Olsson[3]
[1] Vibrometric Oy, Helsinki, Finland
[2] Section for Solid Earth Physics, Department of Geophysics, Uppsala University, Sweden
[3] Conterra AB, Uppsala, Sweden
February 1994

TR 94-04
Final report of the AECL/SKB Cigar Lake Analog Study
Jan Cramer (ed.)[1], John Smellie (ed.)[2]
[1] AECL, Canada
[2] Conterra AB, Uppsala, Sweden
May 1994

TR 94-05
Tectonic regimes in the Baltic Shield during the last 1200 Ma - A review
Sven Åke Larsson[1,2], Eva-Lena Tullborg[2]
[1] Department of Geology, Chalmers University of Technology/Göteborg University
[2] Terralogica AB
November 1993

TR 94-06
First workshop on design and construction of deep repositories - Theme: Excavation through water-conducting major fracture zones Såstaholm Sweden, March 30-31 1993
Göran Bäckblom (ed.), Christer Svemar (ed.)
Swedish Nuclear Fuel & Waste Management Co, SKB
January 1994

TR 94-07
INTRAVAL Working Group 2 summary report on Phase 2 analysis of the Finnsjön test case
Peter Andersson (ed.)[1], Anders Winberg (ed.)[2]
[1] GEOSIGMA, Uppsala, Sweden
[2] Conterra, Göteborg, Sweden
January 1994

TR 94-08
The structure of conceptual models with application to the Äspö HRL Project
Olle Olsson[1], Göran Bäckblom[2], Gunnar Gustafson[3], Ingvar Rhén[4], Roy Stanfors[5], Peter Wikberg[2]
1 Conterra AB
2 SKB
3 CTH
4 VBB/VIAK
5 RS Consulting
May 1994

TR 94-09
Tectonic framework of the Hanö Bay area, southern Baltic Sea
Kjell O Wannäs, Tom Flodén
Institutionen för geologi och geokemi, Stockholms universitet
June 1994

TR 94-10
Project Caesium–An ion exchange model for the prediction of distribution coefficients of caesium in bentonite
Hans Wanner[1], Yngve Albinsson[2], Erich Wieland[1]
[1] MBT Umwelttechnik AG, Zürich, Switzerland
[2] Chalmers University of Technology, Gothenburg, Sweden
June 1994

TR 94-11
Äspö Hard Rock Laboratory Annual Report 1993
SKB
June 1994

TR 94-12
Research on corrosion aspects of the Advanced Cold Process Canister
D J Blackwood, A R Hoch, C C Naish, A Rance, S M Sharland
AEA Technology, Harwell Laboratory, UK
January 1994

TR 94-13
Assessment study of the stresses induced by corrosion in the Advanced Cold Process Canister
A R Hoch, S M Sharland
Chemical Studies Department, Radwaste Disposal Division, AEA Decommissioning and Radwaste, Harwell Laboratory, UK
October 1993

TR 94-14
Performance of the SKB Copper/Steel Canister
Hans Widén[1], Patrik Sellin[2]
[1] Kemakta Konsult AB, Stockholm, Sweden
[2] Svensk Kärnbränslehantering AB, Stockholm, Sweden
September 1994

TR 94-15
Modelling of nitric acid production in the Advanced Cold Process Canister due to irradiation of moist air
J Henshaw
AEA Technology, Decommissioning & Waste Management/Reactor Services, Harwell, UK
January 1994

TR 94-16
Kinetic and thermodynamic studies of uranium minerals. Assessment of the long-term evolution of spent nuclear fuel
Ignasi Casas[1], Jordi Bruno[1], Esther Cera[1], Robert J Finch[2], Rodney C Ewing[2]
[1] MBT Tecnología Ambiental, Cerdanyola, Spain
[2] Department of Earth and Planetary Sciences, University of New Mexico, Albuquerque, NM, USA
October 1994

TR 94-17
Summary report of the experiences from TVO's site investigations
Antti Öhberg[1], Pauli Saksa[2], Henry Ahokas[2], Paula Ruotsalainen[2], Margit Snellman[3]
[1] Saanio & Riekkola Consulting Engineers, Helsinki, Finland
[2] Fintact Ky, Helsinki, Finland
[3] Imatran Voima Oy, Helsinki, Finland
May 1994

TR 94-18
AECL strategy for surface-based investigations of potential disposal sites and the development of a geosphere model for a site
S H Whitaker, A Brown, C C Davison, M Gascoyne, G S Lodha, D R Stevenson, G A Thorne, D Tomsons
AECL Research, Whiteshell Laboratories, Pinawa, Manitoba, Canada
May 1994

TR 94-19
Deep drilling KLX 02. Drilling and documentation of a 1700 m deep borehole at Laxemar, Sweden
O Andersson
VBB VIAK AB, Malmö
August 1994

TR 94-20
Technology and costs for decommissioning the Swedish nuclear power plants
Swedish Nuclear Fuel and Waste Management Co, Stockholm, Sweden
June 1994

TR 94-21
Verification of HYDRASTAR: Analysis of hydraulic conductivity fields and dispersion
S T Morris, K A Cliffe
AEA Technology, Harwell, Didcot, Oxon, UK
October 1994

TR 94-22
Evaluation of stationary and non-stationary geostatistical models for inferring hydraulic conductivity values at Äspö
Paul R La Pointe
Golder Associates Inc., Seattle, WA, USA
November 1994

TR 94-23
PLAN 94
Costs for management of the radioactive waste from nuclear power production
Swedish Nuclear Fuel and Waste Management Co
June 1994

TR 94-24
Äspö Hard Rock Laboratory
Feasibility and usefulness of site investigation methods. Experiences from the pre-investigation phase
Karl-Erik Almén (ed.)[1], Pär Olsson[2], Ingvar Rhén[3], Roy Stanfors[4], Peter Wikberg[5]
[1] KEA GEO-Konsult
[2] SKANSKA
[3] VBB/VIAK
[4] RS Consulting
[5] SKB
August 1994